RC1:

Summary

This study characterizes NPF in a coastal city in China and discusses the NPF contribution to CCN concentration. There is an in depth comparison of how NPF events differ from non-NPF days in terms of the aerosol size distribution, chemical composition/hygroscopicity, and precursor gases. I thought the authors did a good job of discussing their results and explaining how different mechanisms contribute to formation and growth of NPF. My comments are mostly about clarification/the need for additional details about the methods.

Response: We appreciate the time and effort that the editor and the reviewers dedicated to providing feedback on our manuscript. We are grateful for the insightful comments and valuable improvements to our paper. We have incorporated most of the suggestions made by the reviewers. According to your suggestion, we modified the manuscript in detail and marked the revised contents with red font.

Major Comments

1. I would suggest reframing the goal in the (introduction) and outcome (conclusion) of this study away from wording such as "quantification of its ultimate climate effects" (Line 76) and "climatic impact of NPF" (Line 392). While this study does quantify and discuss mechanisms of NPF and their contribution to CCN concentrations, it may be more precise to frame this work as defining the CCN efficiency or cloud nucleating ability of NPF, or the *potential* climatic impact of NPF. Better understanding and representing CCN concentration is an important bridge to understanding their climate effects, but an actual cloud impact due to CCN is not quantified in the paper.

- On this note, it would also be helpful to state more directly at the end of the introduction the primary new aspect of the work. Is it new/unique because of the region specifically? Because of the focus on linking observations to the various

mechanisms? Initially it read to me like the unique aspect was linking NPF to CCN, which the authors recognize in Lines 64-70 has been done in other studies.

Response: We thank the reviewer for this thoughtful and constructive comment. We fully agree that our original wording overstated the direct climate relevance of our findings, and that the novelty of the work was not clearly distinguished from previous studies that have already linked NPF events to increased CCN concentrations. we have made the following revisions:

Line 93-96: However, some studies suggest that an increase in hydrophobic organic components during subsequent particle growth may inhibit CCN generation. Therefore, understanding the role of different components during particle growth is crucial for assessing their subsequent climate effects.

Line 101-104: Currently, understanding how regional variations in atmospheric oxidants and precursors affect the growth of newly formed particles to CCN sizes, especially the quantification of their CCN efficiency, remains a challenge and a frontier in current research.

Line 529-530: This work demonstrates that the potential climatic impact of NPF in coastal urban areas is not simply a function of its occurrence frequency or formation strength.

2. It is specified that the study includes 46 NPF days, but there is no number given for the non-NPF cases. There are many claims made about the differences in NPF and non-NPF conditions in the Supplement figures, and I think that some context needs to be given as to how much more data is being considered in the non-NPF subset compared to the NPF events. For example, if the rest of the full year is included in the non-NPF subset, that could be a large quantitative difference compared to 46 days.

Response: We thank the reviewer for pointing out this missing piece of information. We agree that the number of non-NPF days should be clearly stated to provide proper context for the comparisons shown in Section 2.4.

Line 257-258: During the one-year observation, a total of 46 NPF events and 319 non-NPF days were identified.

3. Additional detail would strengthen the measurement and instrumentation section, especially for the OC/EC analyzer, WPS-1000, AE-33, and chromatograph. For example, not all instruments are given a time resolution, and it is not clear how different observations are combined. Are certain datasets averaged over some time period? How do you combine high resolution in situ aerosol observations with 1-hr meteorological data? What are the uncertainties of each of these observations, and how do these uncertainties impact the analysis/results?

Response: We thank the reviewer for this constructive comment. We have substantially revised the measurement and instrumentation section to provide the missing details. Below, we address each specific point.

Time resolution of each instrument. We have now explicitly stated the native time resolution for each instrument in a new table (Table S1 in the Supplement) and in the revised main text. Specifically, the WPS-1000 provides particle number size distributions every 6 min; the AE-33 Aethalometer measures black carbon at 1 h, but we used 1-hour averaged data; the OC/EC analyzer (Sunset Model-4) produces hourly OC and EC concentrations; and the MARGA (online chromatograph for gases and water-soluble ions) also outputs hourly data. The meteorological data and routine air quality data are both available at 1-hour resolution. All these time resolutions are now clearly indicated in the revised manuscript

Table S1. Summary of measurement instruments, parameters, time resolution, averaging time used for analysis, and measurement uncertainties.

Station	Instrument	Parameter(s)	Time resolution	Uncertainty
The Fujian Provincial Environmental Monitoring Center Station	WPS-1000	Aerosol size distribution (10–350 nm)	6 min	±10%
	AE-33	BC	1 h	±10% (Drinovec et al., 2015)
	OC/EC Analyzer	OC, EC	1 h	OC: ±3.6%; EC: ±6.8% (Zhang et al., 2021)
	MARGA (ADI 2080)	SO_4^{2-}, NO_3^-, NH_4^+, Na^+, K^+, Ca^{2+}, Cl^-; NH_3, HNO_2, HNO_3, HCl, SO_2	1h	±5–20% (Battelle, 2009)

The Fuzhou Meteorological Bureau Station	Meteorological station	T, RH, WS, WD, precipitation	1 h	T: ±0.2°C; RH: ±4–8%; WS: ±(0.5+0.03v) m/s; WD: ±5°; precip.: ±0.4 mm/±4%
	CCNC-100	CCN number concentration and spectrum distribution	10 min per SS	±10%

Reference:

Battelle: Environmental Technology Verification Report: Applikon MARGA Semi-Continuous Ambient Air Monitoring System, U.S. Environmental Protection Agency, available at: https://nepis.epa.gov/Exe/ZyPURL.cgi?Dockey=P100FZOD.pdf (last access: 24 April 2026), 2009.

Drinovec, L., Močnik, G., Zotter, P., Prévôt, A. S. H., Ruckstuhl, C., Coz, E., Rupakheti, M., Sciare, J., Müller, T., Wiedensohler, A., and Hansen, A. D. A.: The "dual-spot" aethalometer: an improved measurement of aerosol black carbon with real-time loading compensation, Atmos. Meas. Tech., 8, 1965–1979, https://doi.org/10.5194/amt-8-1965-2015, 2015.

Zhang, X., Trzepla, K., White, W., Raffuse, S., and Hyslop, N. P.: Intercomparison of thermal–optical carbon measurements by Sunset and Desert Research Institute (DRI) analyzers using the IMPROVE_A protocol, Atmos. Meas. Tech., 14, 3217–3231, https://doi.org/10.5194/amt-14-3217-2021, 2021.

4. Additional details would also strengthen the analysis methods section:

1) The section reads a bit like a list of equations and needs more description of how these tie together and what they will be used for in later analyses.

Response: We thank the reviewer for this constructive comment. We have made the following revisions to Section 2.2

The growth rate (GR) of new particles was calculated following (Kulmala et al., 2012):

$$GR = \frac{\Delta D_m}{\Delta t} \quad (1)$$

where D_m is the median diameter of the nucleation mode particles, obtained by fitting a log-normal distribution to the particle number size distribution. Statistics of the fitting results (see Supplementary Material) demonstrate that the log-normal distribution represents the observed particle size distributions well, with the majority of fits yielding high coefficients of determination (R^2>0.85); only fits with R^2>0.7 were used to avoid propagating poor-fitting uncertainties. GR describes how rapidly particles grow from the nucleation size to larger sizes. It is later used to estimate the formation rate of new particles (Eq. 2) and condensable vapor concentration (Eq. 4) and to evaluate the competition between condensation and coagulation during NPF events.

The condensation sink (CS) reflects the rate at which condensable vapor molecules condense onto the surface of pre-existing atmospheric particles and was calculated as follows (Kulmala et al., 2012):

$$CS = 4\pi D \sum_i \beta_{M,i} \cdot D_i \cdot N_i \quad (2)$$

where D is the diffusion coefficient of the vapor (typically assumed to be sulfuric acid), N_i is the number concentration of particles in a given size bin, and β_M is a correction factor.

The coagulation sink (CoagS) reflects the ability and rate of pre-existing atmospheric particles to remove newly formed nucleation particles via coagulation. For particles of size i, the coagulation sink can be expressed as:

$$CoagS_i = \sum_j K_{ij} N_j \quad (3)$$

where N_j is the number concentration of particles in size bin j, and K_{ij} is the Brownian coagulation coefficient between particles of size j and i.

The formation rate (FR) of new particles was calculated following Kulmala et al. (2012):

$$FR = \frac{dN_{nuc}}{dt} + CoagS_{nuc} \cdot N_{nuc} + \frac{GR}{\Delta dp} + S_{losses} \quad (4)$$

where N_{nuc} is the number concentration of nucleation-mode particles. Following the definition by Kulmala et al. (2012), the nucleation-mode size range in this study was also limited to below 25 nm. $CoagS_{nuc} \cdot N_{nuc}$ is the flux of particles lost due to coagulation with pre-existing particles, where $CoagS_{nuc}$ is the coagulation sink for

nucleation-mode particles. GR/Δdp represents the flux of particles growing out of the nucleation size range (exceeding 25 nm), which is generally negligible under typical atmospheric conditions (Dal Maso et al., 2005). FR is later used to compare NPF event intensity under different meteorological and chemical conditions, and to identify periods with active nucleation. The additional loss term S_{losses} (e.g., dilution due to boundary layer growth, wall losses) was negligible under our field conditions (Dal Maso et al., 2005). For regional NPF events, transport losses can also be ignored. FR is a direct measure of NPF intensity and is later compared across different meteorological and chemical conditions.

Condensable vapor concentration (C) and source rate (Q). Assuming that particle growth is dominated by condensation of a low-volatility vapor (typically sulfuric acid), the vapor concentration can be estimated from the observed growth rate (Dal Maso et al., 2005; Kulmala et al., 2012):

$$C = A \times \frac{dDp}{dt} \quad (5)$$

where D_p is the particle diameter, and A is a constant, which has the value 1.37×10^{-7} $h\cdot cm^{-3}\cdot nm^{-1}$ for a vapor with molecular properties of sulfuric acid (Dal Maso et al., 2005). This provides an upper-limit estimate of the condensable vapor concentration, as it assumes growth is solely due to condensation of the vapor and neglects contributions from coagulation.

The CS (Eq. 2) quantifies the rate at which this vapor is removed by pre-existing particles. Under steady-state conditions (dC/dt=0), the vapor source rate Q can be derived as (Dal Maso et al., 2005):

$$Q = CS \times C \quad (6)$$

This source rate represents the net production of condensable vapor needed to maintain the observed growth and is later compared with precursor gas concentrations (e.g., SO_2) to infer the chemical pathways driving NPF.

Hygroscopicity parameter (κ_{inorg}) for inorganic species. Due to the lack of organic composition measurements, we estimated the hygroscopicity of the inorganic fraction only. The measured water-soluble ions (SO_4^{2-}, NO_3^-, NH_4^+, Cl^-) were converted to mass

concentrations of inorganic salts using the ion-pairing scheme described in Gysel et al. (2007) and Kuang et al. (2020). The following salts and their κ values (Kuang et al., 2020) were considered: $(NH_4)_2SO_4$ (κ = 0.48), NH_4NO_3 (κ = 0.58), NH_4HSO_4 (κ = 0.56), and NH_4Cl (κ = 0.93). The volume fraction of each salt was calculated using its density (also from Kuang et al., 2020). The overall inorganic hygroscopicity parameter κ_{inorg} was then obtained by volume-weighted mixing (Petters and Kreidenweis, 2007):

$$\kappa_{inorg} = \sum_i \varepsilon_i \kappa_i \quad (7)$$

where κ_i and ε_i represent the hygroscopicity parameter and volume fraction of component i in the mixture, respectively, and i denotes the number of components. This K_{inorg} represents the hygroscopicity of the inorganic aerosol components and is used as an upper-limit estimate for the total particle hygroscopicity, as organic matter (typically less hygroscopic) was not included.

The concentrations of secondary organic carbon (SOC) and primary organic carbon (POC) were estimated following (Wu and Yu, 2016):

$$POC = (OC/EC)_{min} \times EC \quad (8)$$

$$SOC = OC_{total} - (OC/EC)_{pri} \times EC \quad (9)$$

where OC_{total} is the measured OC, $(OC/EC)_{min}$ is the minimum (OC/EC) ratio during the observation period, POC is primary organic carbon, and SOC is secondary organic carbon.

The enhancement effect on cloud condensation nuclei number concentration (E_N_{CCN}) was defined as the ratio of CCN number concentration after the NPF event to that before the event (Ren et al., 2021):

$$E\_N_{CCN} = N_{CCN,\,after} / N_{CCN,\,prior} \quad (10)$$

where $N_{CCN,\,after}$, is the average CCN number concentration during the NPF event (from its start to end), and $N_{CCN,\,prior}$, is the average CCN concentration during the 2 h before the event. This factor directly links NPF to potential cloud formation: a value >1 indicates that NPF increases CCN availability.

XGBoost-SHAP framework. To quantitatively evaluate the nonlinear effects of

meteorological factors (temperature, RH) and precursor gases (NH_3, SO_2) on the particle formation rate (FR), we applied an interpretable machine learning framework combining XGBoost (Extreme Gradient Boosting) with SHAP (SHapley Additive exPlanations). A detailed description of the feature selection, model training, validation, and SHAP interpretation is provided in the supplementary material (Text S1). The main quantitative thresholds and interaction strengths derived from this analysis are discussed in Section 3.4.

2) How well does the log-normal distribution fit the observed particle size distributions (Lines 130-131)? How well does the Kulmala et al. (2012) nucleation size mode range apply to observations here (Line 135)? Under what conditions are the last two terms in the FR equation negligible (Line 137)? Does the "overall chemical composition of particles" come from observations (Line 156-157)?

Response: Thanks for your constructive comments. We also recognized a gap in the description of the log-normal distribution fit. We have now added the following content to the supplementary materials:

To ensure high data fidelity for subsequent calculations of growth rate (GR), formation rate (FR), and condensable vapor concentration, a rigorous quality control (QC) protocol was implemented. Only fits satisfying both of the following criteria were retained: (1) $R^2>0.7$, and (2) $N\leq106$ cm^{-3}. The latter criterion serves as a physically constrained upper limit to exclude spurious mathematical solutions arising from instrumental noise or extreme outliers.

As shown in Fig.S1a, the retained fits account for approximately 58% of the total dataset, a robust proportion considering the intermittent nature of new particle formation (NPF) events and the frequent occurrence of low-signal background conditions. The majority of R^2 values lie between 0.85 and 0.95, with a peak near 0.91, indicating that the log-normal model effectively captures the variance of the observed nucleation-mode particles.

Fig. S1b displays the parameter space of the fitted nucleation mode (Dpg vs. N). A high-

density cluster appears at Dpg<10 nm with elevated N, which serves as a definitive signature of NPF events. The observed downward-bending density band reflects the classical aerosol dynamic evolution: a burst of nucleated particles followed by simultaneous diameter growth (increasing Dpg) and sink-driven concentration decay (decreasing N).

The frequency distribution of σ is presented in Fig.S1c. The median σ is approximately 1.7, and most values fall within 1.5–2.0. This is highly consistent with the theoretical expectations for a well-defined, unimodal nucleation mode in atmospheric aerosol physics.

In summary, the log normal distribution provides a statistically robust (high R2), physically meaningful (reasonable D_{pg}-N evolution, σ within 1.5–2.0), and stable representation of the nucleation mode PSDs in our dataset. Fits with R2≤0.7 (e.g., during non-NPF or mixed mode conditions) are excluded from analyses requiring a well-defined nucleation mode.

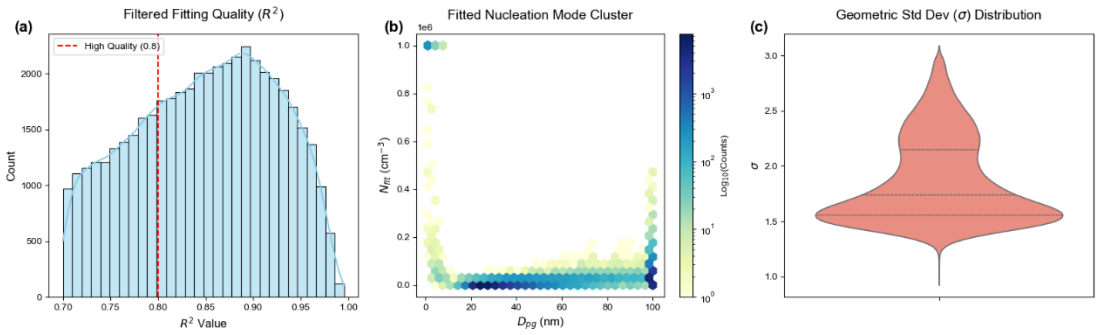

Fig. S1 Evaluation of the single-mode log-normal fitting for nucleation-mode particle size distributions (PSDs). (a) Frequency distribution of the coefficient of determination (R^2) for the retained fits (R^2>0.7). The red dashed line indicates the high-quality threshold of 0.8. (b) Density plot (hexagonal binning) of the fitted nucleation-mode parameter space showing the relationship between geometric mean diameter (D_{pg}) and total number concentration (N). The color scale represents the number of occurrences on a logarithmic scale. (c) Frequency distribution (violin plot) of the retrieved geometric standard deviation (σ). The dashed and dotted lines within the violin plot indicate the median and quartiles, respectively.

Additionally, the overall chemical composition of particles used in this study (including water-soluble ions, OC, EC, etc.) was directly measured by the instruments summarized in Table S1. Specifically, water-soluble inorganic ions (SO_4^{2-}, NO_3^-, NH_4^+, Cl^-, etc.) were measured by the MARGA (online chromatograph), and organic carbon (OC) and elemental carbon (EC) were measured by the Sunset OC/EC analyzer. These observations formed the basis for calculating the hygroscopicity parameter (κ_{inorg}) and estimating secondary organic carbon (SOC).

Table S2. Summary of measurement instruments, parameters, time resolution, averaging time used for analysis, and measurement uncertainties.

Station	Instrument	Parameter(s)	Time resolution	Uncertainty
The Fujian Provincial Environmental Monitoring Center Station	WPS-1000	Aerosol size distribution (10–350 nm)	6 min	±10%
	AE-33	BC	1 h	±10% (Drinovec et al., 2015)
	OC/EC Analyzer	OC, EC	1 h	OC: ±3.6%; EC: ±6.8% (Zhang et al., 2021)
	MARGA (ADI 2080)	SO_4^{2-}, NO_3^-, NH_4^+, Na^+, K^+, Ca^{2+}, Cl^-; NH_3, HNO_2, HNO_3, HCl, SO_2	1h	±5–20% (Battelle, 2009)
The Fuzhou Meteorological Bureau Station	Meteorological station	T, RH, WS, WD, precipitation	1 h	T: ±0.2°C; RH: ±4–8%; WS: ±(0.5+0.03v) m/s; WD: ±5°; precip.: ±0.4 mm/±4%
	CCNC-100	CCN number concentration and spectrum distribution	10 min per SS	±10%

Minor Comments

1. Lines 51-60: What factors govern formation rate and growth rate?

Response: Thank you very much for raising this important point. We will add a clearer explanation in the revised manuscript.

Line 62-67: The availability of precursor vapors and the atmospheric chemical

environment play decisive roles. H_2SO_4 is a key nucleating species, and its stabilizing co-components, such as ammonia (NH_3) and amines, can dramatically enhance FR (Dunne et al., 2016; Yao et al., 2018; Kirkby et al., 2016). For particle growth, condensation of low-volatility compounds is the dominant process. Sipilä et al. (2010) showed experimentally that early-stage growth is primarily driven by H2SO4 condensation.

2. Lines 55-56: How is NPF occurrence constrained by temperature and humidity?

Response: Thank you very much for raising this important point. We will add a clearer explanation in the revised manuscript.

Line 69-78: Low temperatures promote nucleation, whereas high temperatures suppress it (Sipilä et al., 2010; Dunne et al., 2016; Yu et al., 2017). Dunne et al. (2016) further showed that at low temperatures, the ion-enhancement effect is weak due to suppressed evaporation of neutral clusters, while at ambient temperatures, ions can increase the nucleation rate by about a factor of 15. Consequently, neglecting temperature dependence leads to a marked overestimation of NPF and CCN concentrations in summer (Yu et al., 2017). Hamed et al. (2011), based on observations at multiple continental sites, found that NPF events predominantly occur at relative humidity below 60% and are rare above 80%. The reason is that high relative humidity reduces ultraviolet radiation, lowering the production of OH and H_2SO_4; meanwhile, hygroscopic growth enhances the condensation sink, thereby suppressing new particle formation.

Reference:

Dunne, E. M., Gordon, H., Kürten, A., Almeida, J., Duplissy, J., Williamson, C., Ortega, I. K., Pringle, K. J., Adamov, A., Baltensperger, U., Barmet, P., Benduhn, F., Bianchi, F., Breitenlechner, M., Clarke, A., Curtius, J., Dommen, J., Donahue, N. M., Ehrhart, S., Flagan, R. C., Franchin, A., Guida, R., Hakala, J., Hansel, A., Heinritzi, M., Jokinen, T., Kangasluoma, J., Kirkby, J., Kulmala, M., Kupc, A., Lawler, M. J., Lehtipalo, K., Makhmutov, V., Mann, G., Mathot, S., Merikanto, J., Miettinen, P., Nenes, A., Onnela, A., Rap, A., Reddington, C. L. S., Riccobono, F., Richards, N. A. D., Rissanen, M. P., Rondo, L., Sarnela, N., Schobesberger, S., Sengupta, K., Simon, M., Sipilä, M., Smith, J. N., Stozkhov, Y., Tomé, A., Tröstl, J., Wagner, P. E., Wimmer, D., Winkler, P. M., Worsnop, D. R., and Carslaw, K. S.: Global atmospheric particle formation from CERN CLOUD measurements, Science, 354, 1119–1124, https://doi.org/10.1126/science.aaf2649, 2016.

Maso, M. D., Kulmala, M., Riipinen, I., Wagner, R., Hussein, T., Aalto, P., and Lehtinen, K.: Formation and growth of fresh atmospheric aerosols: eight years of aerosol size distribution data from SMEAR II, hyytiälä, finland, Boreal Environ. Res., 2005.

Sipilä, M., Berndt, T., Petäjä, T., Brus, D., Vanhanen, J., Stratmann, F., Patokoski, J., Mauldin, R. L., Hyvärinen, A.-P., Lihavainen, H., and Kulmala, M.: The role of sulfuric acid in atmospheric nucleation, Science, 327, 1243–1246, https://doi.org/10.1126/science.1180315, 2010.

Yu, F., Luo, G., Nadykto, A. B., and Herb, J.: Impact of temperature dependence on the possible contribution of organics to new particle formation in the atmosphere, Atmos. Chem. Phys., 17, 4997–5005, https://doi.org/10.5194/acp-17-4997-2017, 2017.

3. Line 63: Can you be more specific on what the "various atmospheric conditions" refer to?

   Response: Thank you for pointing this out. By "various atmospheric conditions," we meant different environments such as urban, suburban, rural, mountain, and varying levels of pollution. We have clarified this in the revised manuscript.

   Line 87-88: Observations across different sites (e.g., mountain, urban) have shown that NPF events typically lead to a significant increase in N_{CCN} (Kuwata et al., 2008; Yue et al., 2011; Fan et al., 2018).

4. Line 76/77: What exact mechanisms are being referred to here? Different ones than nucleation mechanisms listed in Line 72?

   Response: Thank you for pointing this out. We have made the following revisions:

   Line 101-103: Currently, understanding how regional variations in atmospheric oxidants and precursors affect the growth of newly formed particles to CCN sizes, especially the quantification of their CCN efficiency, remains a challenge and a frontier in current research

5. Line 86-90: It seems like these first two sentences could be combined to be more concise.

   Response: Thank you for your helpful suggestion. We have combined the two sentences in lines 86–90 to improve conciseness.

   Line 114-117: Observation data for this study were collected from June 1, 2021, to May 30, 2022, during comprehensive atmospheric environmental observations conducted at

the Fujian Provincial Environmental Monitoring Center Station (26.11°N, 119.30°E, altitude 65 m) and the Fuzhou Meteorological Bureau Station (26.05°N, 119.26°E, altitude 18 m).

6. Line 103: OPC is not defined. OPC.

Response: Thank you for your helpful suggestion. We have given the complete name.

Line 131-133: To maintain counting accuracy, the instrument was regularly calibrated for T gradient, flow rate, pressure, SS, and the optical particle counter (OPC) using standard ammonium sulfate according to the method by Rose et al. (2008).

7. Line 140: This seems to be a repeat equation in the text.

Response: Thank you for your careful reading of our manuscript. We have correct that the equation presented in line 140 is a repetition.

Line 177-181:

The condensation sink (CS) reflects the rate at which condensable vapor molecules condense onto the surface of pre-existing atmospheric particles and was calculated as follows (Kulmala et al., 2012):

$$CS = 4\pi D \sum_i \beta_{M,i} \cdot D_i \cdot N_i \quad (2)$$

where D is the diffusion coefficient of the vapor (typically assumed to be sulfuric acid), N_i is the number concentration of particles in a given size bin, and β_M is a correction factor.

8. Line 201: Can you clarify that pollution levels were higher on NPF days in spring and winter? From Fig. S3 at first glance it looks like pollution levels are highest in spring and summer.

Response: Thank you very much for raising this important point. We will add a clearer explanation in the revised manuscript.

Line 274-276: It should be noted that the absolute $PM_{2.5}$ and PM_{10} in winter and spring were still relatively high compared to other seasons (Fig. S3), implying that even on NPF days.

Line 280-285: Although winter had heavy background pollution, Fig.S4 shows that the

gaseous precursor SO_2 concentration on NPF days was significantly higher than on non-NPF days (winter: 0.88 vs. 0.76 $\mu g \cdot m^{-3}$; spring: 0.64 vs. 0.53 $\mu g \cdot m^{-3}$). This indicates that in polluted seasons, high gaseous precursors can overcome the inhibitory effect of a high CS and thus trigger nucleation. In contrast, NPF days in summer and Fall exhibited a distinctly clean background, with NH_3 and HNO_2 significantly lower than on non-NPF days (Fig.S4).

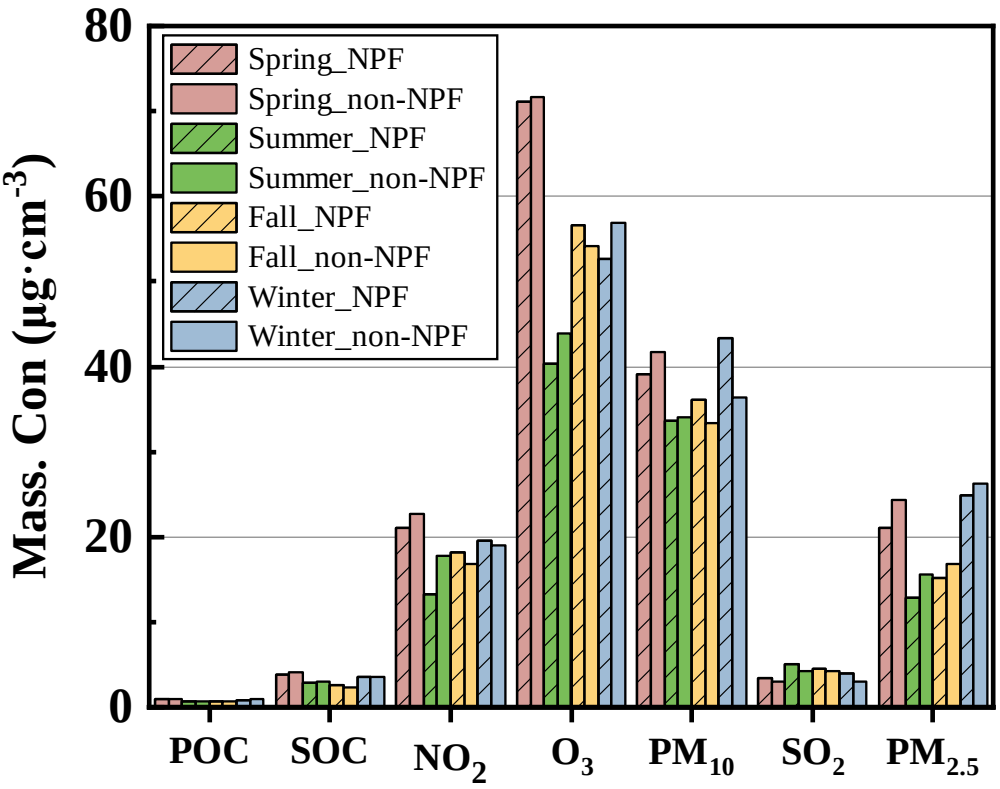

Fig.S3 Mass concentrations of particulate pollutants between NPF days and non-NPF days.

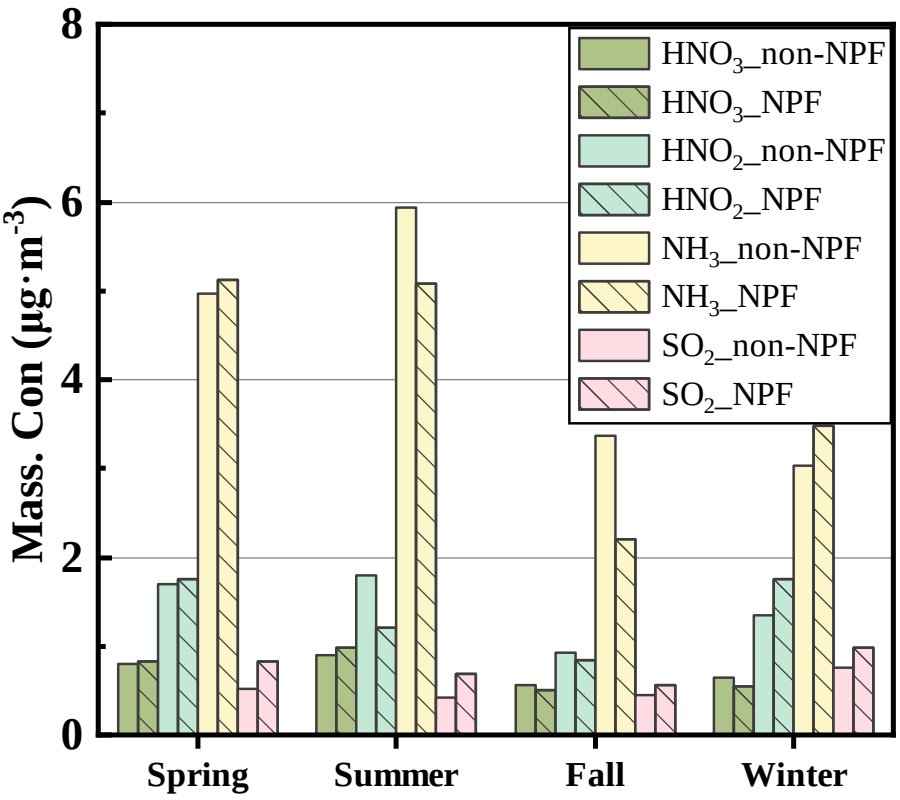

Fig.S4 Mass concentrations of precursor gases (e.g., SO_2, NO_2, O_3, NH_3) between NPF days and non-NPF days.

9. Line 205-206: I am not seeing that secondary organic ion concentrations are similar between NPF and non-NPF days in spring from Fig. S4. Is this a typo?

   Response: Thank you very much for raising this important point. We will add a clearer explanation in the revised manuscript.

   Line 288-292: However, spring presents a special case in that the SNA (sulfate, nitrate, and ammonium) concentrations on NPF days were comparable to those on non-NPF days (SO_4^{2-}: 4.35 vs. 4.27 $\mu g \cdot m^{-3}$). This indicates that spring NPF events are driven by high precursor concentrations. Even when the background particle level is high, the abundant supply of gaseous precursors (Fig. S4) can still overcome the inhibition and trigger NPF events.

10. Line 208-209: Is the hygroscopicity parameter calculated for only nucleation mode particles? Or for all observed aerosols?

    Response: Thank you for raising this important point. In the original manuscript, the hygroscopicity parameter (κ_{inorg}) was calculated for all measured water-soluble

inorganic ions in $PM_{2.5}$, not specifically for nucleation mode particles alone. This represents the bulk aerosol hygroscopicity of the submicron fraction, which includes particles of all sizes (from nucleation to accumulation mode). We agree that the original wording was ambiguous. To clarify, we have added the following sentence in the revised manuscript (Section 2.3, Eq. 7):

Lin 216-228:

Hygroscopicity parameter (κ_{inorg}) for inorganic species. Due to the lack of organic composition measurements, we estimated the hygroscopicity of the inorganic fraction only. The measured water-soluble ions (SO_4^{2-}, NO_3^-, NH_4^+, Cl^-) were converted to mass concentrations of inorganic salts using the ion-pairing scheme described in Gysel et al. (2007) and Kuang et al. (2020). The following salts and their κ values (Kuang et al., 2020, Table S2) were considered: $(NH_4)_2SO_4$ (κ = 0.48), NH_4NO_3 (κ = 0.58), NH_4HSO_4 (κ = 0.56), and NH_4Cl (κ = 0.93). The volume fraction of each salt was calculated using its density (also from Kuang et al., 2020). The overall inorganic hygroscopicity parameter κ_{inorg} was then obtained by volume-weighted mixing (Petters and Kreidenweis, 2007):

$$\kappa_{inorg} = \sum_i \varepsilon_i \kappa_i \quad (7)$$

where κ_i and ε_i represent the hygroscopicity parameter and volume fraction of component i in the mixture, respectively, and i denotes the number of components. This κ_{inorg} represents the hygroscopicity of the inorganic aerosol components and is used as an upper-limit estimate for the total particle hygroscopicity, as organic matter (typically less hygroscopic) was not included.

11. Line 266-267 & Fig. S8: It looks like kappa decreases with time in fall and that there's a small net decrease in spring. Summer appears to be the only season with a substantial increase, but it also oscillates quite a bit. This is explained more in the next paragraph, but it is not immediately clear from Fig. S8 that kappa generally increases following NPF events in the other 3 seasons.

Response: Thank you for your careful observation regarding Figure S8 and the

corresponding explanation in the text.

In response to your comment, and also following a valuable suggestion from another reviewer, we have refined our calculation of κ_{inorg} by including chloride (Cl^-) as an additional inorganic component. The revised κ values and their seasonal variations have been re-analyzed, and the updated figure (originally Fig. S8, now renumbered as Fig. S10) now more clearly demonstrates that κ_{inorg} generally increases after NPF events in all four seasons, although the magnitude of increase varies.

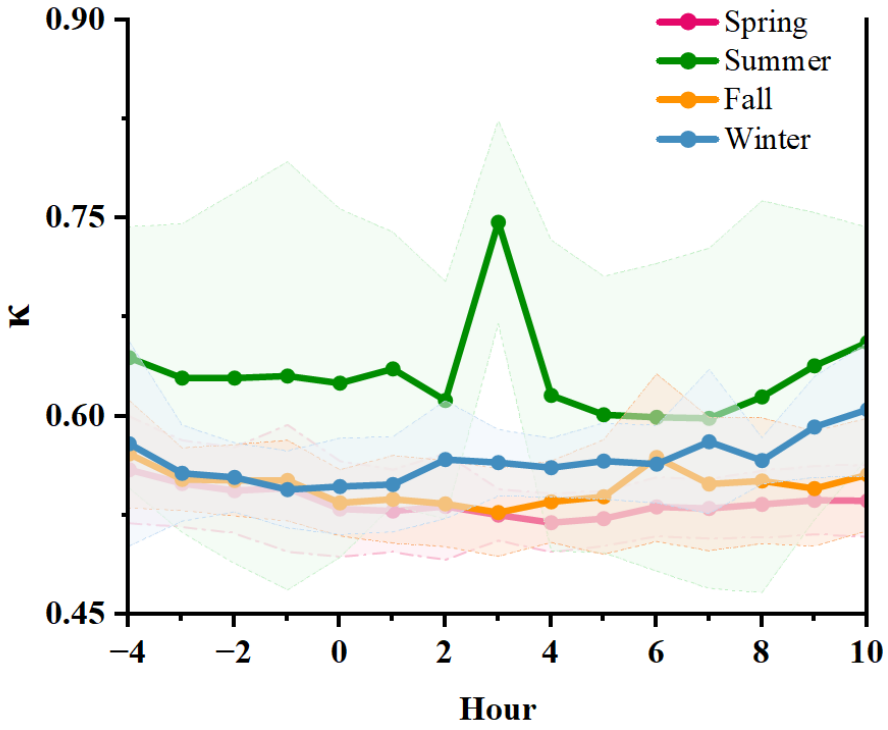

Fig.S10 Temporal evolution of the particle hygroscopicity parameter (κ_{inorg}) during NPF events. The x-axis follows the same normalized time scale as defined in Fig. 4 (t = 0 h represents NPF event start). Shaded bands indicate ±1σ standard deviation.

12. Fig. S9: Would it be possible to put all panels on the same x-axis scale to make it easier to compare differences in magnitude between seasons?

Response: Thank you for this suggestion. We have revised Fig. S9 so that all panels now share the same x-axis scale. This change indeed facilitates a clearer comparison of seasonal differences. The updated figure has been included in the revised manuscript.

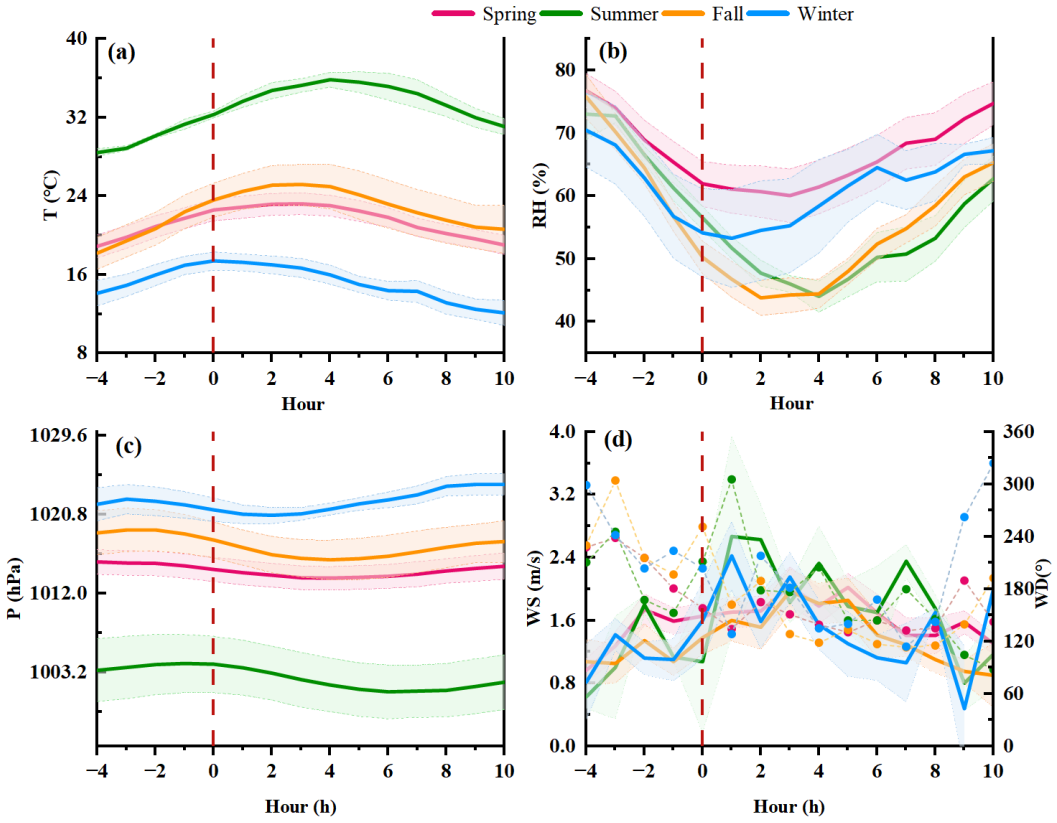

Fig. S11 Temporal evolution of meteorological parameters, including (a) temperature (T), (b) relative humidity (RH), (c) pressure (P), and (d) wind speed (WS, solid lines) and wind direction (WD, dashed lines with dots) during NPF events across four seasons. The x-axis follows the same normalized time scale as defined in Fig. 4, where t = 0 h represents the onset of the NPF event. In panels (a)-(c), solid lines represent the median values, and shaded bands indicate. In panel (d), the left y-axis corresponds to WS, while the right y-axis corresponds to WD.

13. Line 275: This section discusses meteorology in addition to chemistry. Would it make sense to add meteorology into the section title?

Response: We thank the reviewer for the careful reading and the thoughtful suggestion. The section in question (Section 3.3, originally titled "Influence of chemical composition on NPF events") indeed briefly describes meteorological conditions such as temperature, wind direction, and relative humidity as part of the seasonal context. However, the primary focus of this section is to elucidate how the chemical composition of aerosols and precursor gases (e.g., NH_3, SO_2, sulfate, nitrate, BC, POC, SOC) drives

the observed seasonal variations in NPF parameters (FR, GR, CS, etc.). Meteorological variables are mentioned only as background environmental settings that do not constitute the core analytical theme. Adding "meteorology" to the section title would risk overemphasizing their role and potentially misleading readers about the main message of this section. Therefore, we prefer to keep the original title unchanged. We have, nonetheless, clarified in the revised text that meteorological conditions serve as contextual background, while the mechanistic interpretation remains focused on chemical drivers. We hope the reviewer finds this explanation reasonable.

14. Line 350-351: If this section is about spring, I think the reference needs to be changed to Fig. S12a. Also, at SS = 0.4%, I do not see what would be considered a "rapid decline" in CCN from that panel.

Response: Thank you very much for raising this important point. First, regarding the figure citation error, we have corrected it in the revised manuscript. Second, concerning the description of a "rapid decline" at SS = 0.4%: after re-examining the data, we found that the decrease in N_{CCN} at this supersaturation level is indeed modest (approximately 7%), so the wording "rapid decline" was inappropriate. However, at high SS (e.g., 0.8% and 1.0%), the decline is substantially more pronounced (exceeding 25%). To avoid misleading readers, we have revised the text as follows:

Line 483-485: N_{CCN} (0.4 % SS, the same as below) increased from a pre-event average (-4 to -1 h) of about 2636 cm^{-3} to 3192 cm^{-3} at 4 h, then decreased slowly from 4 to 6 h, with a larger decline at higher supersaturations (Fig. S17a).